doi.org/10.36721/PJPS/2026.40.16011.1

Development and *in-vivo* evaluation of dual-drug-loaded transdermal films for prolonged release and improved Alzheimer's therapy

Bariki Rajasekhar[1]* and Haranath Chinthaginjala[2]

[1]Research scholar, Department of Pharmaceutical Sciences, JNTUA, Ananthapuramu-515001 andhra Pradesh, India

[2]Department of Pharmaceutics, Raghavendra Institute of Pharmaceutical Education and Research (RIPER)-Autonomous, K. R. Palli Cross, Ananthapuramu-515721 andhra Pradesh, India, Affiliated to JNTUA, Ananthapuramu-515001 andhra Pradesh, India

Abstract: **Background**: Poor adherence and suboptimal therapeutic results are common challenges in the management of Alzheimer's disease, indicating an urgent need for alternative drug delivery strategies to enhance treatment optimization and patient compliance. **Objectives**: To develop *in-vivo* label transdermal pharmaceutical films containing Memantine (MMT) and Donepezil (DPZ) for improved patient compliance and optimized drug therapy in Alzheimer's disease. **Methods**: The films were prepared with PVP K30, modified chitosan and HPMC K15. Among the various formulations evaluated *in-vitro* and *in-vivo*, the most promising, TDP-11, was selected. Six healthy adult male New Zealand white rabbits were used to assess the drug's availability from the patches; blood samples were collected for pharmacokinetic studies. **Results**: The transdermal patches TDP-1 to TDP-15 displayed uniform weights (115-132 mg) and thickness measurements between 0.22-0.31 mm; The folding endurance reached a range of 160 to 270 and their pH level, which is safe for skin use, measured between 5.7 and 6.5; The swelling capacity reached 165% and their moisture vapor transmission rate ranged from 220 to 450 g/m^2/h. The drug content reached a high level, ranging from 97.5 to 99.8 %, while the substance absorbed moisture at a rate of 91.7 to 99.5 % and lost moisture at a rate of 1.8 to 6.2 %. The TDP-11 patch showed superior performance through its maximum flux of 18.5 µg/cm^2/h and its permeability of 0.07 cm/h, which outperformed both DPZ (3.1±0.05) and MMT (4.2±0.04). Animal testing in 6 rabbits showed that the optimized TDP-11 achieved maximum blood concentration and maximum absorption time at 6 h with complete systemic absorption. **Conclusion**: This investigation shows that the films offer controlled release of the drug. The higher pharmacokinetic parameters of the TDP-11 formulation also suggest that these patches are an attractive and efficient alternative to intact oral drug administration, especially suited for pretension administration.

Keywords: Alzheimer's disease; Delivery; Donepezil; Memantine; Transdermal

Submitted 09-01-2026 – Revised 13-03-2026 – Accepted 06-04-2026

Article in Press

INTRODUCTION

Over several years, Alzheimer's disease (AD) has been an advanced neurological disease and the main cause of Alzheimer's disease (AD) causing consistent memory, thinking, behavior and everyday functioning problems (Milanifard *et al.*, 2025). Abnormal aggregation of amyloid-β and tau proteins in the brain causes neuronal death, synaptic impairment and brain volume loss (Bhushan *et al.*, 2018). Age, genetic factors (APOE 2 allele) (apolipoprotein E gene), traumatic brain injury, cardiovascular conditions and lifestyle are among the established risk factors (Angelopoulou *et al.*, 2021). Though no cure exists, to some extent, symptomatic treatments with dopaminergic precursors, cholinesterase inhibitors, NMDA receptor antagonists and lifestyle modifications can improve symptoms and slow progression (Egunlusi *et al.*, 2024); developing disease-modifying therapies is underway.

Particularly for transdermal patches, a novel dosage form that delivers drugs to the systemic circulation via a controlled-release mechanism through the skin, we study the evolution of transdermal drug delivery systems (TDDS) (Zhang *et al.*, 2024). Transdermal films provide controlled release, are free from gastric irritation, are devoid of first-pass metabolism and are non-invasive (Safiri *et al.*, 2024). The typical components of a transdermal patch are a backing layer, a drug reservoir or matrix, a rate-regulating membrane and an adhesive layer, which together help drug absorption through the skin to be successful. With drugs needing long-term treatment, they are quite popular and include nicotine in smoking cessation, nitroglycerin in angina, fentanyl in pain management and hormones in hormone replacement therapy (Aminisaman *et al.*, 2025). Experiments are ongoing to increase their effectiveness by using permeation enhancers, new polymers and nanotechnology-based compression solutions to overcome the inherent barrier properties of the stratum corneum (Koppa Raghu *et al.*, 2020).

Because they offer significant advantages over oral treatments, transdermal patches for the treatment of AD are gaining increasing popularity. Low oral bioavailability, gastrointestinal adverse effects and administration difficulties associated with swallowing difficulties in

**Corresponding author:* e-mail: barikirajasekar@gmail.com

elderly individuals account for a major share of the medicines used in AD, including rivastigmine and donepezil (Scheltens *et al.*, 2021). Transdermal patches improve patient compliance with a single daily or multi-day application; provide steady, controlled drug delivery; bypass first-pass metabolism; and reduce side effects associated with peaks. By simply peeling off the patch, they also facilitate termination, thereby ensuring it is safe in case of side effects. Particularly for elderly patients and those with poor cognition in need of long-term Alzheimer's therapy, transdermal patches thus provide a practical and effective means of drug distribution (Matsunaga *et al.*, 2018).

Since they determine the efficiency of medication absorption from the skin into the systemic circulation, thereby exerting a therapeutic impact, bioavailability studies are essential for transdermal patches used in AD. Since Alzheimer's medicines, including rivastigmine, galantamine and donepezil, have low and very variable oral bioavailability- that is, decreased bioavailability and high first-pass metabolism- as well as gastrointestinal perturbation, transdermal delivery is being explored to get around these drawbacks. Still, skin is quite a strong barrier and the extent of medication penetration may vary depending on the formulation design, the condition of the patient's skin and the site of application. Bioavailability studies are required to ensure that transdermal patches are at least as effective as oral equivalents, are released in a controlled manner and provide consistent plasma levels. The studies are also crucial for evaluating patch-to-patch variation, adhesion and safety to determine whether the method enhances clinical efficacy and lowers adverse effects in Alzheimer patients (Winblad *et al.*, 2006).

The present study introduces its first original contribution by creating an optimized drug formulation that combines Memantine and Donepezil, two different anti-Alzheimer drugs that doctors prescribe together in clinical practice. Memantine decreases glutamate-induced brain damage by blocking NMDA receptors; Donepezil boosts cholinergic neurotransmission by inhibiting acetylcholinesterase, which breaks down acetylcholine. The developed system implements a QbD framework by defining the Quality Target Product Profile, identifying Critical Quality Attributes, Critical Material Attributes and Critical Process Parameters and optimizing them through statistical design to achieve controlled release, uniform drug distribution, mechanical stability and reproducible performance, thereby improving robustness and scalability over trial-and-error methods. The innovative element of the research enables two drugs with different physicochemical properties to coexist within a single delivery system while maintaining proper drug compatibility and synchronized release, minimizing peak-to-trough fluctuations and delivering continuous therapeutic effects. The *in-vivo* pharmacokinetic tests confirmed that the treatment led to increased systemic absorption, extended half-life and greater bioavailability, thereby establishing a significant connection between the *in-vitro* and *in-vivo* results. The formulation improves Alzheimer's treatment through its dual-mechanism therapy, which scientists developed according to QbD principles and confirmed through biological tests in a single, patient-friendly dosage form that boosts medication adherence while enhancing treatment outcomes compared to traditional multidose regimens.

Still, regarding the given material, the main objective of this work was to evaluate the *in-vivo* characteristics of transdermal patches containing Donepezil (DPZ) and Memantine (MMT). The general goal was to increase drug treatment for people with AD, who often forget to take their oral medications daily and to improve patient compliance. Using optimized patches in a rabbit model, the study sought to regulate the pharmacokinetic parameters and bioavailability of the medicines following administration.

MATERIALS AND METHODS

Materials

Cipla Limited, Bengaluru, India, donated donepezil (120014-06-4) and memantine (19982-08-2); Fischer Scientifics bought HPMC K15 (9004-65-3), altered chitosan (9012-76-4), PVP K30 (9003-39-8), dichloromethane (75-09-2) and propylene glycol (57-55-6); SD Fine chemicals supplied acetonitrile and o-phosphoric acid, as well as HPLC-grade triple glass distilled water and analytical-grade chemicals. Wistar rabbits (New Zealand) for the *in-vivo* investigation were supplied by Ambika Animal Farms in Bengaluru. The *in-vivo* investigation adhered to the Animal Ethical Guidelines for Laboratory Investigations. Permission from the Institutional Animal Ethics Committee (RIPA/2020/COL-19R) was sought for experimentation. For conducting animal experiments, CPCSEA (No. 855/ac/05/CPCSEA/009/2021) has approved the institution.

Trial batch

Via the one-factor-at-a-time (OFAT) method, preliminary test formulations of MMT and DPZ transdermal patches were produced. Originally evaluated were three polymers, as per previous studies: hydroxypropyl methylcellulose (HPMC) K 15 M (50 to 200 mg), modified chitosan (50 to 200 mg) and PVP K 30 (10 to 100 mg). Subsequently, the most appropriate concentrations were established (HPMC K 15M in the range of 100 to 150 mg, modified chitosan in the range of 100 to 200 mg and PVP K 30 in the range of 30 to 50 mg), which determined the following formulation optimization relying on a Box-Behnken design (BBD) that is a statistical Quality by Design (QbD) technique (Ahad *et al.*). This allowed us to study the interaction effects of the polymers in greater detail and to create an optimal

Article in Press

formulation with desirable transdermal properties (Javed *et al.*, 2022).

To prepare the polymeric solution, HPMC K 15M and modified chitosan were separately dissolved in dichloromethane. A cosolvent/plasticizer/permeability enhancer, PVP K 30, was added to improve homogeneity of the mixture and to provide flexibility in the patch. A polymeric solution was prepared to which DPZ and MMT were added and the mixture was left to stand as entrapped air was removed over 1 h. Sonication was also used to further remove air bubbles (Kumar *et al.*, 2023).

The solution was prepared and then poured into a folded square-shaped aluminum foil (10x10 cm). The rectangular patches, 2x2 cm with 20 mg of DPZ and MMT, were cut after drying and peeled off. It was assembled using aluminum foil as a backing membrane, to which medical adhesive tape was applied, allowing adhesion to the skin (Sailaja *et al.*, 2025). The wax paper was used to cover the drug-loaded surface up to the time when the patch is to be used. Every formulation was fabricated by solvent casting (Table 1) and the composition of various formulations is shown in table 2.

Calibration curve

The DPZ and MMT were combined to make a stock solution of 1 mg/mL in methanol. 10 mL volumetric flasks containing such a stock were thereafter diluted with phosphate-buffered saline (PBS), pH 7.4, to yield a final concentration of 0.2 to 0.8 µg/mL. Using a double-beam UV-visible spectrophotometer (Shimadzu-1800) at pH 7.4 PBS, which served as the blank, the absorbance of each diluted solution was recorded at 269 nm (Nunes *et al*., 2024). A calibration curve was created by plotting absorbance versus DPZ/MMT concentration (DPZ/MMT). Estimations of DPZ/MMT concentrations in unknown samples were made using these values. The determination coefficient (r^2) was used to determine the linearity of the standard curve.

Physical compatibility test

The thermal compatibility of DPZ and MMN with selected excipients to be used in formulation development was determined using Differential Scanning Calorimetry (DSC). Thermograms of unadulterated drugs, individual excipients and physical mixtures of the drugs with the excipients were taken using a DSC apparatus. The physical mixture was heated to 30-300°C. The crystalline nature of DPZ and MMN was evidenced by sharp endothermic peaks noted at their melting points in the DSC thermograms of the two compounds (Sharma *et al.*, 2018). The presence, absence, or change in the 5 peaks in the drug-excipient mixtures was studied in detail (Kharia *et al.*, 2020).

Chemical compatibility test

Fourier Transform Infrared (FTIR) spectroscopy was utilized to assess the compatibility of DPZ and MMN with the formulation excipients. FTIR spectra of different drugs in their pure form, as well as individual excipients and their physical mixtures, were measured under the KBr pellet method at 4000-400 cm^{-1}. Their spectra had distinguishing absorption peaks connecting to functional groups of DPZ and MMN, MMN- stretching N-H stretching C=O and C-N vibrations, among others. Functional group peaks of DPZ and MMN were not significantly shifted, missing, or appearing as new in any of the foremost functional groups across mixtures in drug-excipient spectra, indicating that no chemical communication occurred (Yadav *et al.*, 2017). This validates these results and shows that DPZ/MMN is not mismatched with the excipients selected for making the formulation.

Evaluation of the patches

Physical appearance

To ensure that the patches look and feel the right way, how the patches appear, how easily they flex, how homogeneous they appear and how smooth they feel, with or without air bubbles and undissolved drug particulates, were monitored by examining the prepared patches. These traits are valuable because they influence the likelihood that a patient will accept a patch and how the patient would respond to it (Bacskay *et al.*, 2023).

Weight consistency

The weight uniformity was ensured to be within the appropriate range for each patch. Took 10 patches at random and weighted. The mean weight is then obtained and the variation of the individual patch weight from the average is expressed. The weight of the patches must be even to ensure that the content in each patch provides the same amount of medicine (Momin *et al.*, 2025).

Thickness

Determining the thickness of the patches with the aid of a fine-grain digital caliper. To measure the thickness of each patch, 3 measurements were taken at different locations within an area of 2x2 cm and averaged to obtain the final thickness of that given area. The procedure above was followed on all patches. Multiple measurements will assist us in having a closer estimation of the thickness. The regularity of thickness among patches is also necessary to smooth and consistent delivery of the medicine (Davanço *et al.*, 2024). This was a measure that enabled us to choose patches with our desired thicknesses.

Folding endurance

This test was run to assess how flexible this was and how long the patches could withstand folding to determine this. This was a test of how many folds it would take for a patch to break. Folding endurance is a decent measure of quality because skin patches need to remain intact at some point during use, removal and wear (Ghosh *et al.*, 2025). This examination enabled us to spot areas strong enough.

Article in Press

Table 1: Various inputs and outputs used in the study.

Independent variables	Levels		
	(-1)	(0)	(+1)
X1= HPMC K15 (mg)	100	125	150
X2= Modified chitosan 80 (mg)	100	150	200
X3= PVP K30 (mg)	30	40	50
Distorted values	-1	0	+1
Y1= DDP@8h (Donepezil permeation at 8 h)	Maximize		
Y2= DDP@16h (Donepezil permeation at 16 h)	Maximize		
Y3= DDP@24h (Donepezil permeation at 24 h)	Maximize		
Y4= MDP@8h (Memantine permeation at 8h)	Maximize		
Y5= MDP@16h (Memantine permeation at 16h)	Maximize		
Y6= MDP@24h (Memantine permeation at 24h)	Maximize		

Table 2: Different formulae made in the study.

Trials	DPZ (mg)	MMT (mg)	HPMC K-15M (mg)	Modified chitosan (mg)	PVP K30 (mg)	DCM (mL)	PG (mL)
TDP-1	20	20	100	100	30	10	1
TDP-2	20	20	150	100	30	10	1
TDP-3	20	20	100	200	30	10	1
TDP-4	20	20	150	200	30	10	1
TDP-5	20	20	100	100	50	10	1
TDP-6	20	20	150	100	50	10	1
TDP-7	20	20	100	200	50	10	1
TDP-8	20	20	150	200	50	10	1
TDP-9	20	20	82.9552	150	40	10	1
TDP-10	20	20	167.045	150	40	10	1
TDP-11	20	20	125	65.9104	40	10	1
TDP-12	20	20	125	234.09	40	10	1
TDP-13	20	20	125	150	23.1821	10	1
TDP-14	20	20	125	150	56.8179	10	1
TDP-15	20	20	125	150	40	10	1

TDP: Transdermal patch; DPZ: Donepezil; MMT: Memantine; PG: Propylene glycol; DCM: Dichloromethane; PG: Propylene glycol

Tensile strength

The tensile strength of the prepared film was determined using a Universal Testing Machine (UTM). The film specimens were cut into strips with standard dimensions of 2 × 5 cm and the thickness of each strip was measured at three locations using a digital micrometer to calculate the average thickness. The film strip was then fixed between the upper and lower grips of the apparatus with an initial gauge length of about 3–5 cm, ensuring no wrinkles or slack. The instrument was operated at a constant cross-head speed (5 mm/min) until the film broke. The film broke when the researchers recorded the required force to break it and they calculated the tensile strength by dividing the maximum load at break by the film's cross-sectional area, which was determined by its thickness and width. The researchers took three measurements for each sample and reported the average with the standard deviation (Sabareesh *et al.*, 2024).

Surface pH

The pH of the patches on the skin surface was determined to establish compatibility with the skin. One patch was placed in a Petri dish containing distilled water and kept in place to swell against the skin-moisture interaction by the same method (30 minutes). Later, the pH was determined with a pH meter. Ideally, a surface pH near 5.5 is appropriate, as it corresponds to the natural body pH at which healthier skin is observed (Kajal *et al.*, 2024). This evaluation was critical for identifying formulations that are not expected to cause skin irritation.

Swelling index

The swelling was assessed to determine its capability for liquid absorption. First, patches were weighed, placed in a mesh assembly and placed in PBS (pH 6.8). The patches were then weighed after specified and fixed periods, after which they were wiped dry with a towel and later reweighed at regular intervals until the weight did not increase further (S. Kim *et al.*, 2024). Rheological features of swelling affect adhesive properties, suppleness and drug release pattern of the patches (Eq. 1).

$$Swelling\ Index\ (\%) = \frac{\text{Final weight} - \text{Initial weight}}{\text{Initial weight}} X100 \quad (1)$$

Article in Press

Moisture vapor transmission

The moisture vapor transmission rate of the patches was determined to assess their moisture-permeation barrier performance. 1g of $CaCl_2$ was placed in a desiccator and a porous plate was placed above an open vial containing a pre-weighed transdermal patch. An adhesive was then placed over the vial mouth and a transdermal patch was applied and left to dry for 5 minutes. The vials were reweighed daily for 7 days (Qadir *et al.*, 2025). The weight gain clarified the moisture distribution across the patch, which explained its permeability and protection.

Drug content uniformity

Content uniformity of the drugs inspected was assessed to determine the overall distribution of the active pharmaceutical ingredient on the patches. Exact cuts of 2 x 2 cm varieties of the patches were accurately cut and dissolved in PBS (pH 7.4). This mixture received uninterrupted shaking overnight to ensure the extraction of all the drugs (Buck *et al.*, 2024). Any insoluble material was removed, after which the amount of the drug in the resulting solution was assessed spectrophotometrically at 269 nm. The absorbance was measured to determine the drug content on the patch and it was also found to be uniform in drug loading.

% Moisture uptake

The moisture uptake of the patches was determined as percentage moisture uptake to assess how they absorb moisture from the atmosphere. To start, the patches were placed in a desiccator and dried for 24 h to remove any pre-existing moisture. The dried samples were placed in a saturated potassium chloride solution in a humidity chamber that maintained a relative humidity of 84% (Ertas *et al.*, 2023). The patches were left in the chamber until the equilibrium weight had been obtained (Eq. 2).

$$Moisture\ uptake\ (\%) = \frac{\text{Final weight} - \text{Initial dry weight}}{\text{Initial dry weight}} X100 \quad (2)$$

% Moisture loss

To determine the patches' ability to retain moisture, the percentage of moisture loss was calculated. Scraps of all formulation batches of three patches were first weighed before recording their initial weight (Wi). These films were placed in a desiccator containing anhydrous $CaCl_2$ and incubated for 3 days at 37°C (Wong *et al.*, 2023). The films were reweighed after this time to obtain the final weight (Wf). The moisture loss as a percentage was determined employing Eq. 3.

$$Moisture\ loss\ (\%) = \frac{\text{Wi} - \text{Wf}}{\text{Wi}} X100 \quad (3)$$

Steady-state flux and drug permeability

Steady-state flux (Jss) is the continual rate of drug transport/flux through a membrane (dialysis membrane MWCO 14kDa), after the inception of a time lag when the steady state occurs, with membrane permeability parameters not subjected to any perturbation(E. J. Kim *et al.*, 2021). It is also the most important parameter in the assessment of the performance of the TDDS since it expresses the rate of drug introduction into the blood through the skin. The permeation studies allow defining a steady-state flux that is found with the help of Eq. 4.

$$\text{Steady state flux} = \frac{\text{Amount of drug permeated through the membrane}}{(\text{Effective surface area of the membrane exposed to the drug}) - (\text{time interval})}$$

Jss may also be determined from the gradient of the straight line on the graph when the plot of the aggregate quantity of drug that has permeated/time is plotted on the straight-line section of that graph. The time to reach the steady-state permeation is centred on the lag time, which is the x-intercept of this linear segment. The steady-state flux is used in an equation to determine the permeability coefficient (Kp), which reflects the drug's capacity to penetrate the skin. It is computed with the help of Eq. 5.

$$\text{Permeability coefficient} = flux/Initial \quad (5)$$

In-vitro permeation

A Franz diffusion cell with a cellulose membrane (soaked in distilled water overnight) was used, which mimics human skin. The patch was kept in the donor section facing the membrane with its drug-facing side. PBS at pH 7.4 and 37°C, to match physiological conditions, was placed in the receptor section. The sampling was done through the receptor section and sink conditions were maintained using fresh PBS (Shivalingam *et al.*, 2021). The samples were then assessed to determine the quantity of the drug that had permeated the membrane.

Drug release kinetics

To determine the mechanism of drug release, the *in-vitro* drug release from the film was analyzed using kinetic models: zero-order, first-order, Higuchi and Korsmeyer-Peppas. The fitting of the discharge data to these models enabled evaluation of the change in drug release and determination of the most likely release mechanism. The major reason is that the most appropriate model describing the data can provide insight into the mechanism of drug release in the patch system, which would be valuable for designing patch characteristics and behavior (Altun *et al.*, 2021; Lei *et al.*, 2022). Since each model corresponds to a different release behavior of a drug, this analysis can be used to identify which mechanism best fits the observed release behavior.

Animal care and monitoring

All animals used in the study were handled and maintained according to IAEC standards and relevant CPCSEA guidelines and to ensure the welfare of the animals at all times. Appropriate measures were taken to reduce pain, suffering and distress. Animals were acclimatized prior to the start of the experimental procedure. Animals were

Article in Press

housed in a controlled environment and provided with environmental enrichment and with food and water ad libitum throughout the study. Temporary fasting was applied before procedure according to protocol. During procedures, animals were handled carefully and blood samples obtained in order to minimise animal stress and discomfort. The animals were observed for adverse effects at intervals appropriate to the nature of the observation and according to relevant CPCSEA guidelines. The species, age, sex and body weight were taken into account. These observations are in respect of changes in general appearance, behaviour, food consumption, water consumption, activity, body weight and conditions of local irritation, if applicable. Particular attention was given to post dosage and post blood sampling conditions. No adverse effects were recorded in this study. The following humane endpoints were applied in the event of severe or persistent pain or distress, severe general deterioration, animal was unable to access water or food, severe local reaction or any other circumstance that was deemed incompatible with continued participation in the study. Had it occurred, the animal would have been removed from the study and treated according to IAEC-approved procedures. It was not felt necessary to establish an additional humane endpoint at this time.

Protocol

A study protocol was written prior to the execution of the in-vivo pharmacokinetic studies. The protocol included information regarding the study objectives, study animals, allocation, treatment of animals, blood sampling times, sample analysis, pharmacokinetic analysis, animal observation and study procedures. The study was undertaken according to the study protocol approved by the Institutional Animal Ethics Committee (IAEC) (RIPA/2020/COL-19R) and in accordance with CPCSEA guidelines. The study protocol was not prospectively registered in a publicly accessible database.

Skin irritation observations

The whole rabbit was regarded as the experimental unit in a study on skin irritation. To assess dermal tolerability of the optimized transdermal patch, healthy adult rabbits were employed. One treated site per rabbit was used to assess the skin tolerability of these patches, whereby the skin was inspected at pre-specified time intervals for inflammation and redness, oedema and other skin reactions. One independent animal contributed one data set for each skin irritation assessment. These are required to determine whether the prepared transdermal patches irritate or sensitize the skin when in constant contact. The animal model was 6 healthy male New Zealand White rabbits weighing 1.8-2.0 kg. The study followed all the protocols set by the college's Animal Ethics Committee. The protocol guaranteed adherence to the ethical and regulatory prescriptions for the humane treatment of animals. There were no food or water restrictions in the study. The animals, prior to treatment, were randomized into four groups of n = 6 each: a control group (shaven skin without treatment), a group with an adhesive bandage, a group with formalin and a group with the optimized formulation (Falcone *et al.*, 2017). All six rabbits were shaved in the center of the back and two patches (TDP-11), each 2x2 cm, were attached to the side and secured with a strip of adhesive tape. One of the two patches contained the drug under study (TDP-11), whereas the other was a drug-free placebo. The animals were observed for 48 h, after which their erythema, edema, sensitization, or allergic reaction was noted. The scale runs from 0 (no irritation) to 4 (severe irritation), allowing one to compare skin compatibility across different experimental conditions fairly. Establishing the safety of the patch in clinical use makes this assessment extremely important (Jiang *et al.*, 2019).

SEM studies

Surface morphology of films before and after their application was investigated by a scanning electron microscope (SEM). Before and after drug release, high-resolution images of the patch on the skin surface were captured using a microscope. Surface structure and polymer matrix changes caused by drug diffusion were observed through a comparative analysis of scanning electron micrographs. The aforementioned observations provide useful information on the drug release process and the physical changes occurring in the patch system during use. The advantages of SEM include its applicability as an analytical technique for elucidating drug-release mechanisms and for assessing alterations in the structure of transdermal patches over time (Singh *et al.*, 2016).

Ex-vivo skin permeation studies

The experiments were conducted in the abdominal skin of Hartley guinea pigs by excision followed by *ex vivo* skin permeation. The animals were euthanized and the abdominal skin was carefully removed to use in the study. Still, all experimental procedures carried out on animals were conducted in accordance with the Institutional Animal Ethical Committee protocol. The detached skin was shaved to expose the skin and positioned between the donor and receptor sides of a Franz diffusion cell with the stratum corneum facing the donor.

The transdermal patch formulation TDP-11 was applied to the donor side and PBS at pH 7.4 was added to the receptor section with a magnetic stir bar. The receptor phase was maintained at 37 °C and agitated continuously to simulate physiological conditions for the receptor (Otterbach *et al.*, 2021). The system was set to withdraw samples at specific times and an equal volume of fresh PBS was added to maintain constant volume. UV spectrophotometry was performed on the collected samples at 269 nm to determine the quantity of drug. TDP-11 was chosen for the permeation experiment because of its favorable *in-vitro* drug release profile in prior investigations using cellulose

Article in Press

nitrate membranes, as well as other desirable physicochemical characteristics. The research is made possible through the assessment of the rate and magnitude of drug inflow into the excised skin, which provides an indication of the transdermal patch's *in-vivo* performance in a predictive manner.

Accelerated stability studies

Stability is an important variable in a TDDS, as it affects drug efficacy and patient adherence. To evaluate the long-term stability of the optimized film (TDP-11), a test patch was wrapped in aluminum foil and stored at 40±2°C and 75±5% RH for 6 months. The patches were examined for physical appearance and uniform drug content at predetermined intervals (days 5, 10, 15, 20, 25 and 30). UV spectrophotometry was used to quantify drug content using the same method that was adopted earlier. The ability to store under different temperatures allowed evaluation of stability to temperature and the effect the environment has on the formulation form. Such an assessment is necessary to help determine the optimal storage conditions and forecast shelf life (Parhi *et al.*, 2018). An important parameter used to test formulation stability is the physical form and drug content, as these ensure the patch remains stable in terms of efficacy, safety and quality.

In-vivo studies

Single animal was the animal experimental unit in the *in-vivo* pharmacokinetic study. Healthy adult rabbits were randomly allocated to each treatment group and dosed with the test formulation as per the study protocol. Blood samples were obtained from each animal at scheduled time points and plasma drug concentrations were determined for each rabbit, from which pharmacokinetic parameters were calculated from the mean concentration-time data of each rabbit, which was used as the independent experimental unit in the statistical analysis. Human dose is 5mg/Average weight of a human (70kg), i.e., 0.07 mg/kg. This was a conversion to animal equivalent dose (AED) in rabbits using a correction factor of 3.1, resulting in an AED of 0.221 mg/kg. The exact AED was estimated per rabbit and relative to body weight. The dose of DPZ/MMT in the final optimized transdermal patch was adjusted accordingly. In the oral group, 5 mg DPZ/ MMT tablets obtained by direct compression of the same polymer mixture used for the transdermal patches were powdered and an equivalent dose (as compared to AED) was administered. To administer orally, the powdered tablet was mixed with water using an altered syringe to reduce the risk of retention in the mouth or dilution from spitting. In the transdermal group, there was the application of one patch to shaved rabbit skin. Skin irritation assessment profiles across oral and transdermal groups were equal in magnitude (Khire *et al.*, 2014). Blood samples thus acquired were stored for up to 48 h, centrifuged and the plasma was stored at sub-zero temperatures until sampling. Acetonitrile was added to precipitate proteins during sample preparation and the mixture was vortexed and centrifuged. This was obtained as a supernatant, which was then evaporated under nitrogen, reconstituted in the mobile phase and tested by reverse-phase high-performance liquid chromatography (RP-HPLC) using UV detection at 269 nm. The relative bioavailability and pharmacokinetic profiles of the two delivery systems were compared by plotting the plasma concentration-time profiles after administration by mouth and by the transdermal system. This comparison will be important to establish the competency of the transdermal patch as an alternative to oral DPZ/MMT tablets.

In - vivo bioavailability studies

In the *in-vivo* pharmacokinetics, six healthy male New Zealand White rabbits weighing 2.25 to 2.5 kg were used and all animal work was carried out in accordance with ethical principles and the institutional guidelines for the care and use of animals. The main objective was to investigate the systemic absorption and pharmacokinetics of the drug following transdermal administration. Before the start of the study, the rabbits were fasted for 10 ± 1 h, with water freely available (ad lib.). All the rabbits were scrubbed at a shaved site on the dorsal area and given a properly placed TDP-11 transdermal patch, ensuring proper drug delivery and low variability. Then, a proper ear vein or marginal vein was carefully accessed and a blood sample (0.5 mL) was collected at predefined time points over 7 days (Day 0 to Day 7) and immediately aliquoted into heparinized microcentrifuge tubes (Akhlaq *et al.*, 2016). The whole blood was then centrifuged at 4,000 rpm for 15 minutes to isolate plasma. The plasma samples acquired were transferred into clean Eppendorf tubes with utmost care and left at -20°C till further analytical quantification. The drug plasma level was subsequently measured and quantified using an HPLC assay (Fig. 1).

Approximation of DPZ and MMT in plasma

The HPLC was employed and the HPLC-grade acetonitrile, o-phosphoric acid and triple-distilled water were used to estimate DPZ and MMT in plasma samples. The pure DPZ and MMT were dissolved in the mobile phase to prepare standard stock solutions at 1 mg/mL for each drug and working standard solutions were generated by diluting the stock solutions to create a calibration curve over a concentration range of 15-90 mg/mL. To prepare the sample, a powdered form of the same portion of the drug patches (1 mg/mL) was dissolved using the mobile phase in a 10 mL volumetric flask and sonicated with the mobile phase (15 minutes). Finally, it was diluted to obtain a final working sample (60 µg/mL) (Bai *et al.*, 2014). The analysis was performed on a Shimadzu HPLC system with LC Solutions software installed, using a Phenomenex Luna C18 column. The mobile phase used was a mixture of acetonitrile and water in a 60:40 volume ratio. The pH of the mobile phase was adjusted to 3.0 with 0.1% o-phosphoric acid and the flow rate was maintained at 1.0 mL/min.

Article in Press

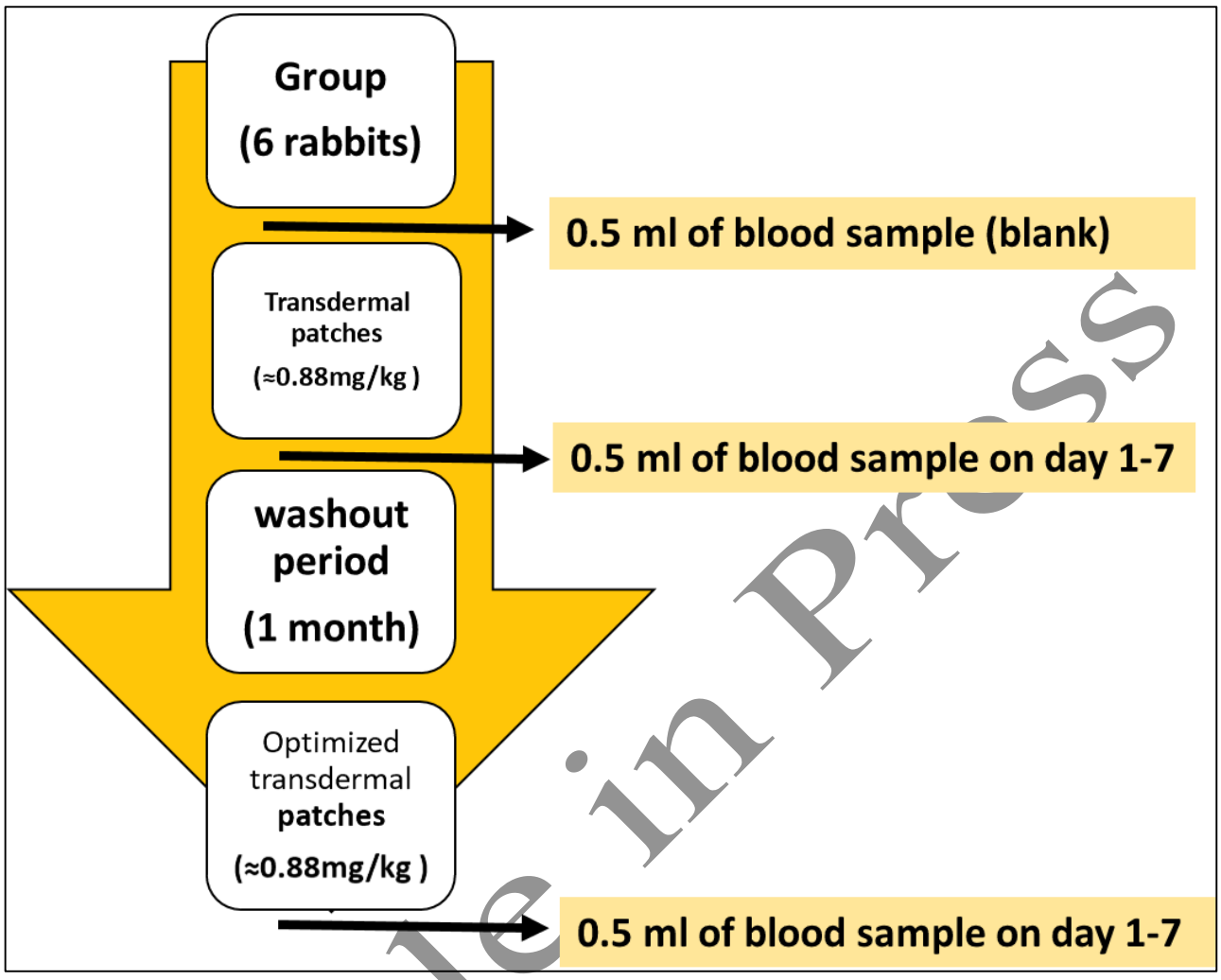


Fig. 1: Animal dosing and the sampling timings for the *in-vivo* investigation
Note: 0.5 mL of blood was collected from the animal. Allowing the samples to clot, then performing centrifugation at 5000 rpm, plasma parting was done. Plasma was then detached to dry tubes and kept in a chilled condition before analysis. The levels of DPZ and MMT in samples were resolved by HPLC.

With an injection volume of 20 µL and a run time of 10.0 minutes, DPZ and MMT were detected using a UV-Vis spectrophotometer at 271 nm and 208 nm, respectively.

Plasma sampling and pharmacokinetics

The analysis of plasma samples was performed by estimating DPZ and MMT using the HPLC procedure described by Amena *et al*. (2015). The sample preparations were performed using 250 µL of rabbit plasma, an internal standard solution of 50 µL and 10 µL of the drugs, with 2 mL acetonitrile in a 10 mL centrifuge tube. The HPLC was then loaded with a 10 L aliquot of the supernatant, followed by centrifugation at 3200 rpm for 10 minutes. The separation was achieved by expanding the method using a mobile phase comprising 60:40 (v/v) of 0.1% o-phosphoric acid buffer and acetonitrile, under which the method performed excellently. Optimum peak resolution was achieved at a 1.0 mL/min flow rate. The chromatographic specification was optimized to achieve a 10-minute run and the detection wavelengths were 271 nm and 208 nm, corresponding to DPZ and MMT, respectively, with native compound interference eliminated. Based on the time vs. plasma concentration data, some pharmacokinetic parameters were deduced (Arora *et al.*, 2002). The calibration curves were used to determine the concentrations of C_{max} (the highest level). This gave a slope of the linear regression line fitted to a semi-log plot of the elimination phase data, the Kel and then entering this approximation into the formula $t ½ = 0.693/K_{el}$ generated the biological half-life (t½) estimate. A value of absorption rate constant (Ka) and percent absorbed was assessed with the Wagner-Nelson equation. The trapezoidal rule was next used to determine the Area under the Curve (AUC).

Article in Press

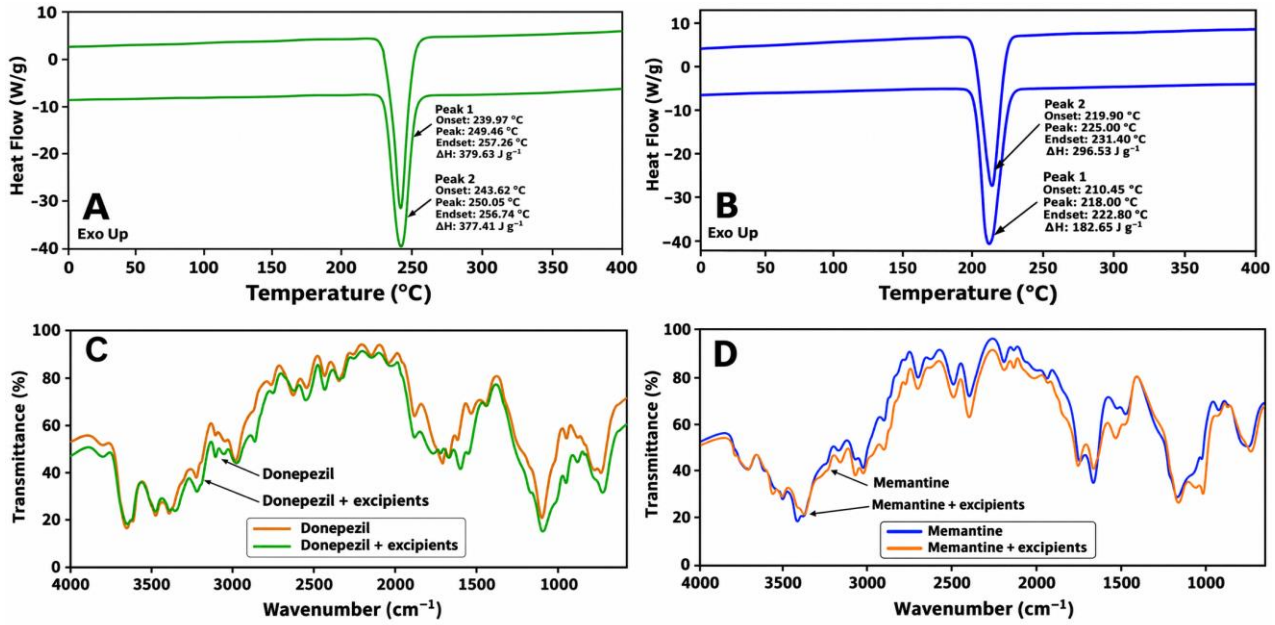


Fig. 2: (A) DSC thermogram of donepezil and its excipient blends; (B) DSC thermogram of the memantine and its blend with the excipients; (C) FTIR spectra of donepezil and donepezil–excipient mixture demonstrating functional group integrity and compatibility; (D) FTIR spectra of memantine and memantine–excipient mixture indicating characteristic absorption bands and absence of significant chemical interaction.

Statistical analysis

They were checked using various statistical measures that analyzed the influence of the controlling factors on the responses, including linear, quadratic, interactive and polynomial terms. Where the p-value of a factor was less than 0.1 (p> 0.1), it was said to have a significant effect.

The non-essential ones (p > 0.1) were excluded from the regression model to simplify it. The increase or decrease in response to a change in the level of the component or variables influencing the component of that word was indicated by a positive or negative coefficient, respectively. The validity of the experimental plan was measured using ANOVA, R^2 and modified R^2. The high R^2 and adjusted R^2 indicated that the model fit the data well.

RESULTS

Calibration curve

The absorbance vs. concentration calibration plot for DPZ gave a straight line described by the regression equation y=0.52x−0.001, confirming that excellent linearity exists between 0.2–0.8 µg/mL. The relatively low intercept indicates that systematic errors due to the solvent and excipients are very low in this concentration range. For MMT, the calibration plot once again showed excellent linearity with the same regression equation as for donepezil: y=0.85x−0.02. The thermogram (Fig. 2A) showed an endothermic peak at 225 ºC for DPZ and at 221 ºC for the drug-excipient combination. In the thermogram (Fig. 2B), pure MMT gives a distinct melting peak at about 230 °C, while there is a very broad and significantly lower peak, around 219 °C, for the MMT-excipient combination, implying a slight interaction or better dispersion of the drug into the excipient matrix. Different absorption bands are visible in the spectrum of pure DPZ designation A, as it shows a strong absorption band due to stretching of the C-H bond at 2950 cm^{-1}, around 1700 cm^{-1} corresponds to the stretching of carbonyls, around 1600 cm^{-1} corresponds to the vibration of aromatic C=C bonds and further stretching of C-N/C-O bonds near 1250 cm^{-1} (Figs. 2 C and 2D). When DPZ is mixed with excipients, those peaks are still observed at almost the same wavenumbers, with only minor intensity changes, indicating the excipients have no effect on the drug's chemical structure. Pure MMT shows several broad absorption bands between 2800 and 3000 cm^{-1}, which can be ascribed to N-H and C-H stretching, as well as a distinct peak around 3300 cm^{-1} and characteristic fingerprint-region signals of an aliphatic amine. The MMT-excipient mixture has preserved these significant bands at the same wavenumbers; it closely matches the fingerprint profile of the pure drug, with only marginal peak broadening, most likely arising from overlaps with excipient contributions.

Physicochemical assets

In relation to the films produced, it should be noted that they were applied uniformly and had smooth, flexible surfaces devoid of cracks, which gave no sign of drug crystallization, signaling good film formation in all formulations. The weight (≈115-132 mg) and thickness (≈0.22-0.31 mm) indicate fairly narrow ranges and further support good reproducibility of the casting process and minimal chances of dose variation.

Article in Press

Table 3: Physicochemical assets of DPZ and MMT transdermal patches

Batch	visibility	Weight (mg)	Thickness (mm)	Folding endurance (number)	Tensile strength (kg/cm²)	Surface pH	Swelling index (%)	Moisture vapor transmission (g/m²/hr)	Drug content (%)		% Moisture uptake	% Moisture loss	Steady-state flux (µg/cm²/h)	Permeability coefficient (cm/h)
									DPZ	NSD				
TDP-1	Smooth, transparent	120.5±1.2	0.25±0.01	210±15	0.85±0.05	6.2±0.1	150±10	350±25	98.5±0.5	95.3±1.2	4.5±0.2	3.1±0.1	12.3±0.8	0.05±0.005
TDP-2	Smooth, opaque	125.1±0.9	0.28±0.02	185±10	1.1±0.10	6.5±0.2	120±8	280±20	99.1±0.4	95.1±3.6	5.8±0.3	4.2±0.2	10.5±0.7	0.04±0.003
TDP-3	Flexible, translucent	118.9±1.5	0.22±0.01	250±20	0.95±0.08	6.0±0.1	165±12	410±30	97.8±0.7	95.7±6.4	6.2±0.4	5.5±0.3	15.8±1.0	0.06±0.006
TDP-4	Matte, opaque	130.4±1.1	0.30±0.01	170±12	1.2±0.10	5.8±0.2	110±5	250±15	98.9±0.6	95.2±8.7	3.9±0.2	2.8±0.1	9.2±0.6	0.03±0.004
TDP-5	Smooth, off-white	122.7±1.0	0.26±0.02	200±15	1.0±0.07	6.3±0.1	135±9	320±22	98.2±0.5	91.7±6.8	5.1±0.3	4.0±0.2	14.1±0.9	0.055±0.005
TDP-6	Opaque, light yellow	128.8±1.3	0.29±0.02	190±13	1.15±0.09	6.1±0.2	128±10	295±18	99.5±0.3	93.2±5.9	4.9±0.2	3.5±0.1	11.8±0.7	0.045±0.004
TDP-7	Clear, smooth	115.3±1.0	0.23±0.01	225±18	0.9±0.06	6.4±0.1	145±11	380±28	98.0±0.6	94.1±2.4	5.4±0.3	4.8±0.2	13.5±0.8	0.052±0.005
TDP-8	White, flexible	132.0±1.4	0.31±0.02	160±10	1.3±0.12	5.9±0.2	105±6	220±15	99.3±0.4	93.7±7.2	3.5±0.2	2.5±0.1	8.7±0.5	0.035±0.003
TDP-9	Transparent, matte	126.5±1.2	0.27±0.01	205±14	1.05±0.08	6.2±0.1	140±10	330±25	97.5±0.8	94.2±3.9	6.0±0.4	5.1±0.3	16.9±1.1	0.065±0.007
TDP-10	Smooth, cream-colored	121.8±1.0	0.24±0.01	215±16	0.98±0.07	6.3±0.2	155±13	360±26	98.7±0.5	93.1±4.4	4.8±0.2	3.7±0.2	12.8±0.9	0.051±0.004
TDP-11	Optimal, translucent	120.0±0.5	0.25±0.05	270±5	1.0±0.05	6.4±0.1	140±5	450±10	99.8±0.1	99.5±2.5	2.5±0.1	1.8±0.1	18.5±0.5	0.07±0.002
TDP-12	Flexible, translucent	117.5±1.4	0.23±0.01	240±19	0.92±0.06	6.5±0.1	160±12	400±30	98.3±0.6	94.2±5.8	5.7±0.4	4.5±0.2	15.0±1.0	0.058±0.006
TDP-13	Smooth, off-white	124.6±1.1	0.27±0.01	195±14	1.1±0.09	6.4±0.2	130±8	310±22	99.2±0.4	99.2±0.4	5.0±0.3	3.9±0.2	11.2±0.7	0.042±0.003
TDP-14	Clear, smooth	127.3±1.2	0.28±0.02	175±12	1.18±0.10	5.7±0.2	100±5	240±18	98.6±0.5	98.6±0.5	3.7±0.2	2.6±0.1	9.5±0.6	0.037±0.003
TDP-15	Flexible, white	123.0±1.0	0.25±0.01	230±17	1.03±0.07	6.2±0.1	148±11	340±24	97.9±0.7	97.9±0.7	5.3±0.3	4.2±0.2	14.5±0.9	0.054±0.005

TDP-11 was selected as the best as it has good physical integrity, optimal pH, high drug content uniformity, and a high steady-state flux.

Surface pH values ranged from 5.7 to 6.5, which is close to the physiological skin pH and has a lower potential for irritation upon application. Mechanical analysis showed satisfactory results for all batches, with folding endurance values exceeding 170 and tensile strengths in the range of 0.85-1.3 kg/cm². Films could be sufficiently flexible to handle mechanical stress, as shown by the above results.

The swelling index (close to 100-165%) and the water vapor transmission rate (almost 220-450 g/m²/h) tended to ensure that an adequate amount of water was absorbed, while moisture exchange was controlled to keep it in contact with the skin without causing excessive swelling or occlusion of the area. The uniformity of drug content was maintained at high levels (97.5-99.8%), ensuring a homogeneous dispersion of DPZ within the polymer matrix. The values for moisture absorption and loss were quite moderate (absorption = 2.5-6.2% and loss = 1.8-5.5%), indicating that low hygroscopicity is thus preventing possible fragility or stickiness during storage. Transdermal performance varied across formulations, with TDP-11 exhibiting the highest steady-state flux of 18.5 µg/cm²/h and permeability coefficient of 0.07 cm/h, indicating a much higher potential for enhanced transdermal delivery of the drug. The physicochemical properties of DPZ and MMT transdermal patches are shown in table 3.

In-vitro drug permeation studies

The simultaneous estimation of DPZ and MMT was found at 269 nm (Fig. 3). All formulated films indicated drug permeation and cumulative permeation with time (Fig. 4A and 4B), where most formulations had a final cumulative mean permeation of about 40-60% at around 240 h. This indicates that the faster drug release and enhanced transport through the skin were compared with other formulations.

Drug release kinetics

Fig. 5A shows the first-order kinetic model, which represents the linear relationship between log percentage residual time. Compared to the straight line, a reasonable linear trend is observed with moderate deviations, with a correlation coefficient close to 0.93, indicating that release does not obey first-order kinetics completely but rather partially. In contrast to this, figure 5B-the Higuchi model indicates a rather high linear correlation between cumulative percentage drug released and the square root of time ($R^2 \approx 0.95$), indicating that diffusion is the most important mechanism underlying the drug release from the polymeric matrix hydrated with solvent. Figure 5C (Korsmeyer-Peppas model) is such that it draws a line between log% drug released and log time with $R^2 \approx 0.96$, such that anomalous (non-Fickian) transport is implied, where both diffusion and polymer relaxation/swelling play their roles in drug release. In figure 5D (Hixson-Crowell model), the highest linearity ($R^2 \approx 0.997$) is obtained in the plot of cube-root fraction of drug remaining versus time, thus indicating that the major role in controlling release from the patch is occupied by changes in surface area as well as by matrix erosion/dissolution.

The first-order kinetic plot (Fig. 6A), i.e., the log percentage remaining vs. time plot, shows an acceptable level of linearity ($R^2 \approx 0.95$). This suggests that the release process is, to some extent, concentration-dependent. Greater linearity in comparison to zero-order kinetics and a mean release time of approximately 13 h corresponds to Fickian drug release, which occurs by diffusion and follows Higuchi (Fig. 6B). The calibrated format of the Korsmeyer-Peppas plot (Fig. 6C) exhibited excellent linearity with the highest correlation coefficient ($R^2 \approx 0.99$) for log percentage drug released versus log time, thus indicating that transport is anomalous (non-Fickian), governed by a damped combination of diffusion and polymer relaxation or swelling. In fact, the Hixson-Crowell plot (Fig. 6D) correlating time with the cube root of the fraction of drug remaining shows relatively low linearity, suggesting that changes in surface area or matrix erosion play only a minor role in the overall release process.

Skin irritation studies

1 h after patch application, during which both erythema and edema scores were 0, it was confirmed that the immediate patch application did not provoke a detectable external inflammatory response. By 24 h, very slight reactions were observed with erythema and edema scores of 0.5 and 0.2, respectively, corresponding to a mean irritation score of 0.35±0.15, which lies within the "barely perceptible" range. At 48 h, erythema and edema had reduced still further to 0.3 and 0.2, producing a mean score of 0.25±0.05, whereas by 72 h the mean score had fallen to 0.05±0.05, evidently indicating almost complete resolution of any temporary response. At all-time points under consideration, the scores remained far below 1 on a 0–4 scale, corroborating the general absence of significant irritation. Permission from the Institutional Animal Ethics Committee (RIPA/2020/COL-19R) was sought for experimentation. For conducting animal experiments, CPCSEA (No. 855/ac/05/CPCSEA/009/2021) has approved the institution. The prepared films were free from skin irritation, as expressed in table 4 and figure 7.

SEM studies

The manufactured transdermal patches have a smooth, uniform surface, a prerequisite for a successful transdermal drug delivery system. The optimized formulation is indicated by this morphological feature, which facilitates the diffusion of active pharmaceutical ingredients, DPZ and MMN, from within the polymeric matrix to the skin surface. Having such pores would be critical in providing the receiving behavioral aspect, especially sustaining and holding drugs for an extended period (Fig. 8A and 8B).

Article in Press

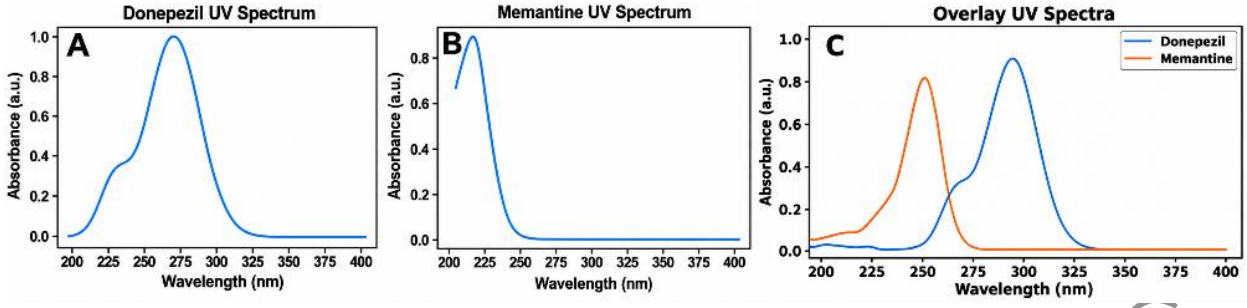


Fig. 3: The UV spectrum of (A) DPZ; (B) MMT and (C) overlay

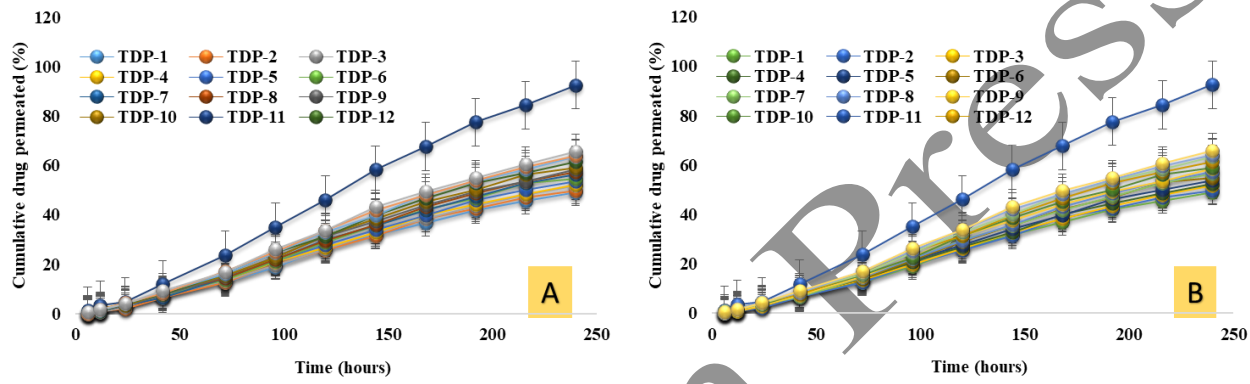


Fig. 4: The *in-vitro* permeation of (A) DPZ and (B) MMT from the transdermal patches

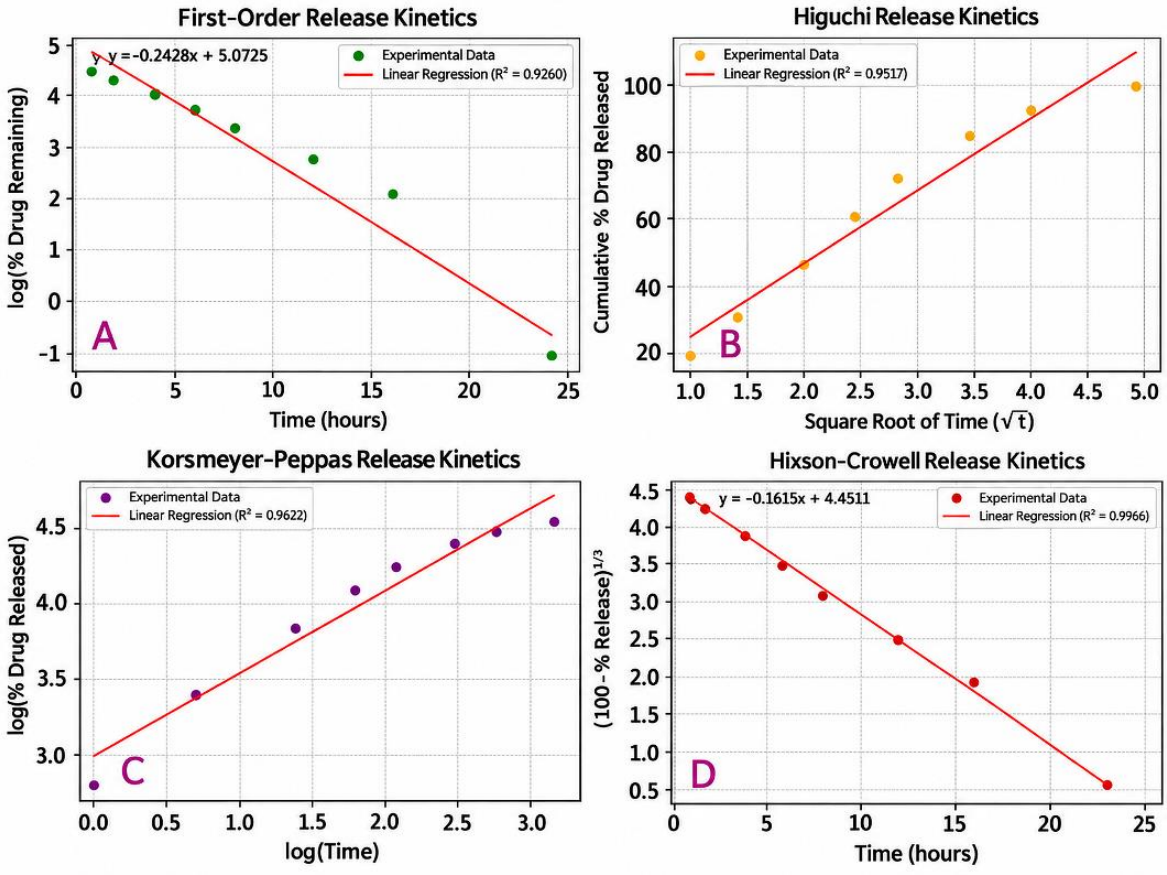


Fig. 5: The drug release kinetics plots from the DPZ from the transdermal patches

In Press

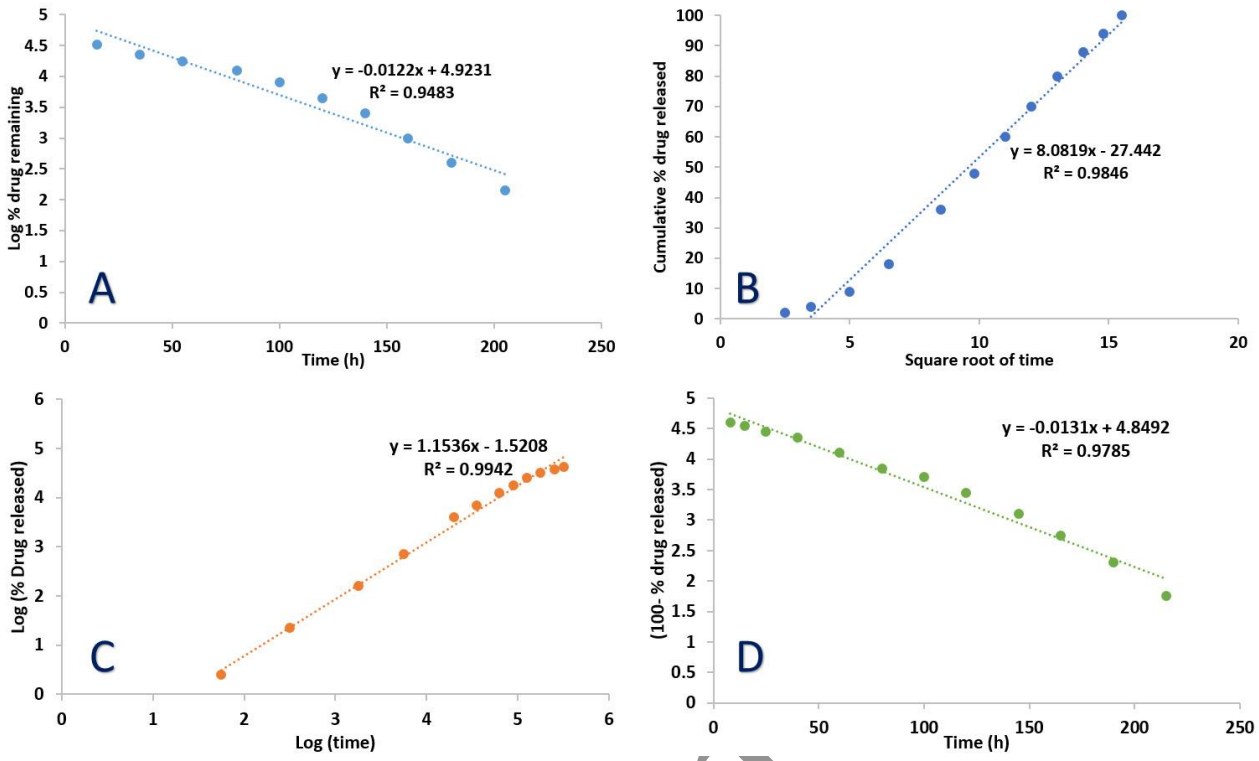


Fig. 6: The drug release kinetics plots from the MMT from the transdermal patches.

Table 4: The skin suitability of transdermal patches is represented by the production of erythema and edema

Time (h)	Erythema	Edema	Mean
1 h	0	0	0.0
24 h	0.5	0.2	0.35±0.15
48 h	0.3	0.2	0.25±0.05
72 h	0.1	0.0	0.05±0.05

score = 0-4



Fig. 7: The study tested skin irritation potential by applying the maximum dose to the rabbit dorsal surface while the animals were held in controlled restraint

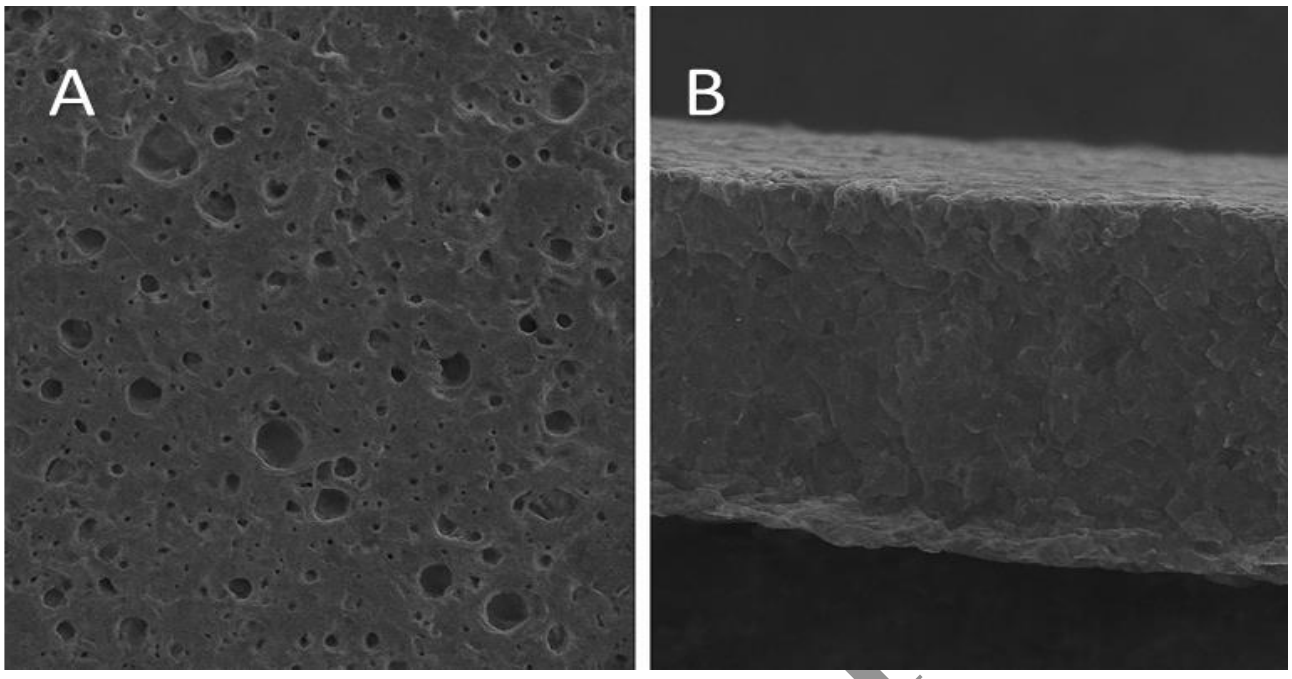


Fig. 8: SEM images of transdermal patches (TDP-11) at (A) 1000 and (B) 500 magnification

Accelerated stability studies

The stability data presented in Table 5 are an important parameter for the long-term sustainability of the transdermal patches. The minuteness of variations in all the parameters measured over half a year during heated conditions is a strong indication that the formulated patches are physically and chemically stable. The uniform weight and thickness mean minimal moisture absorption and minimal structural deterioration, which will not affect the product's quality or dosage.

However, the most important discovery is a high proportion of drug content uniformity. This indicates that the formulation is effective in inhibiting the degradation of DPZ and MMN, thereby delivering a consistent, accurate dose to the patient throughout the product's shelf life. The discovery is a significant voice in favor of the prospective commercial and clinical use of these transdermal patches as a predictable substitute for orally administered medications for Alzheimer's patients. The resultant placed on the swab continued to possess its physicochemical properties even under stressed storage conditions (Table 5).

In-vivo results of TDP-11

The chromatograms show the plasma concentration of TDP-11 over the 7 days after use of the transdermal patch. Day 1 (Fig. 9) shows that TDP-11 is quickly distributed into systemic circulation with a clearly defined chromatographic peak, indicating that the kinetics of initial release of the drug (TDP-11) are tied to the patch. The retention times are consistent over the following days, demonstrating stability in the detection of these drugs without significant interference from plasma components. The slight variations in peak area at this time could be due to patch sticking or to the dynamics of skin permeation. In the final days, from the fifth to the seventh, a slowly decreasing peak in the area indicates a decrease in the rate of drug release as the patch approaches depletion. Throughout the 7 days, the lack of secondary peaks or shifts in retention time points to the absence of detectable metabolites or degradation products of drugs in the examined context.

The chromatographic results are informative regarding the pharmacokinetics of the TDP-11 transdermal patch. The immediate release on Day 1 is typical of transdermal delivery systems and provides rapid attainment of the therapeutic level of the drug. The work carried out indicates that the drug reservoir patch is deficient by Day 7, in line with the reduction in peak area throughout the wear period. These findings support the definition of the patch as a once-weekly dosage form. The consistency of the retention times obtained over the seven days indicates the specificity of the analytical method for the detection of TDP-11, whereas the absence of any interfering peaks supports the selectivity of the assay for the parent compound.

Plasma levels of DPZ from TDP-11

TDP-11 post-application plasma concentration profiles were analysed to ascertain the bioavailability of donepezil and its major pharmacokinetic parameters.

Data obtained on plasma concentration-time profiles after transdermal application of the test formulation were used to plot the pharmacokinetic parameters, most importantly, the AUC and the Area under the First Moment Curve (AUMC). The trapezoidal rule was used to calculate pharmacokinetic parameters.

Article in Press

Table 5: The physicochemical properties of the films were stable even at stressed storage conditions

Sampling time (days)	Physical appearance	Weight consistency (mg)	Thickness (mm)	Folding endurance (number)	Tensile strength (kg/cm²)	Surface pH	Swelling index (%)	Drug content uniformity (%)	
								Donepezil	Memantine
0	Optimal, translucent	120.0±0.5	0.25±0.05	270±5	1.0±0.05	6.4±0.1	140±5	99.8±0.1	99.5±2.5
30	Optimal, translucent	119.8±0.2	0.25±0.01	265±4	0.99±0.02	6.5±0.1	141±8	98.3±0.6	99.2±1.2
60	Optimal, translucent	120.1±0.3	0.25±0.01	268±3	1.10±0.05	6.4±0.2	145±5	99.2±0.4	99.1±2.7
90	Optimal, translucent	120.2±0.5	0.26±0.02	260±2	1.11±0.07	6.2±0.3	138±4	98.6±0.5	99.7±1.4
180	Optimal, translucent	119.7±0.6	0.24±0.01	272±4	1.00±0.02	6.3±0.2	140±3	97.9±0.7	99.2±0.9

The AUC $_{(0\text{-}168)}$ calculated value was 9235.86 µg•hr/L/L, representing the overall systemic exposure of the drug over the 168 h sampling period. This long AUC indicates effective, long-term drug release and absorption through the transdermal system, in line with achieving prolonged therapeutic plasma levels of the drug.

The respective AUMC $_{0\text{-}168}$ was calculated to be 826064.64 µg h^2 /L, which is the total drug exposure time x time and provides details regarding the mean residence time (MRT) of the drug in circulation.

The characteristics of controlled release are rising plasma levels for up to 72 h, followed by a slow drop. At about 72 h, show their highest level, as anticipated in the sustained-release transdermal approach. The decrease over more than 72 h also offers proof of the medicine's long-term absorption and night-by-night excretion.

These findings show that the transdermal patch formula is an effective means of introducing the medicine into the systemic circulation and maintaining drug plasma levels for an extended period, thereby reducing the need for very frequent dosing and enhancing patient adherence (Fig. 10).

The elimination rate constant (Kel) was calculated to be 0.02238 h^{-1}, which is equal to the biological half-life (t½) of 30.97 h. This prolonged half-life demonstrates the viability of maintaining a stable plasma concentration via the transdermal route, leading to reduced administration frequency and reduced repeated dosing (Table 6).

DISCUSSION

Given the linearity across the concentration levels tested for both curves, the analytical conditions used are consistent with the Beer-Lambert law and thus justify simple linear regression for quantitative purposes. The presence of single, well-defined melting endotherms for both drugs in the mixtures, close to those of the pure components, speaks to their thermal compatibility with the selected excipients.

These findings imply that the excipients used in the formulation probably do not adversely affect the stability of DPZ and MMT in the solid state during processing and storage. In this regard, therefore, the DSC data support the suitability of the selected combination of excipients for the development of combined or individual dosage forms of these drugs, whereas the need for further solid-state and stability analyses to confirm the nonexistence of deleterious interactions is clearly justified.

Individual profiles of the characteristic FTIR peaks of DPZ and MMT in excipients indicate that chemical incompatibility or structural modification has not occurred, as the observed individual variation in peak intensity can be attributed to acceptable physical interactions within the polymer matrix.

Article in Press

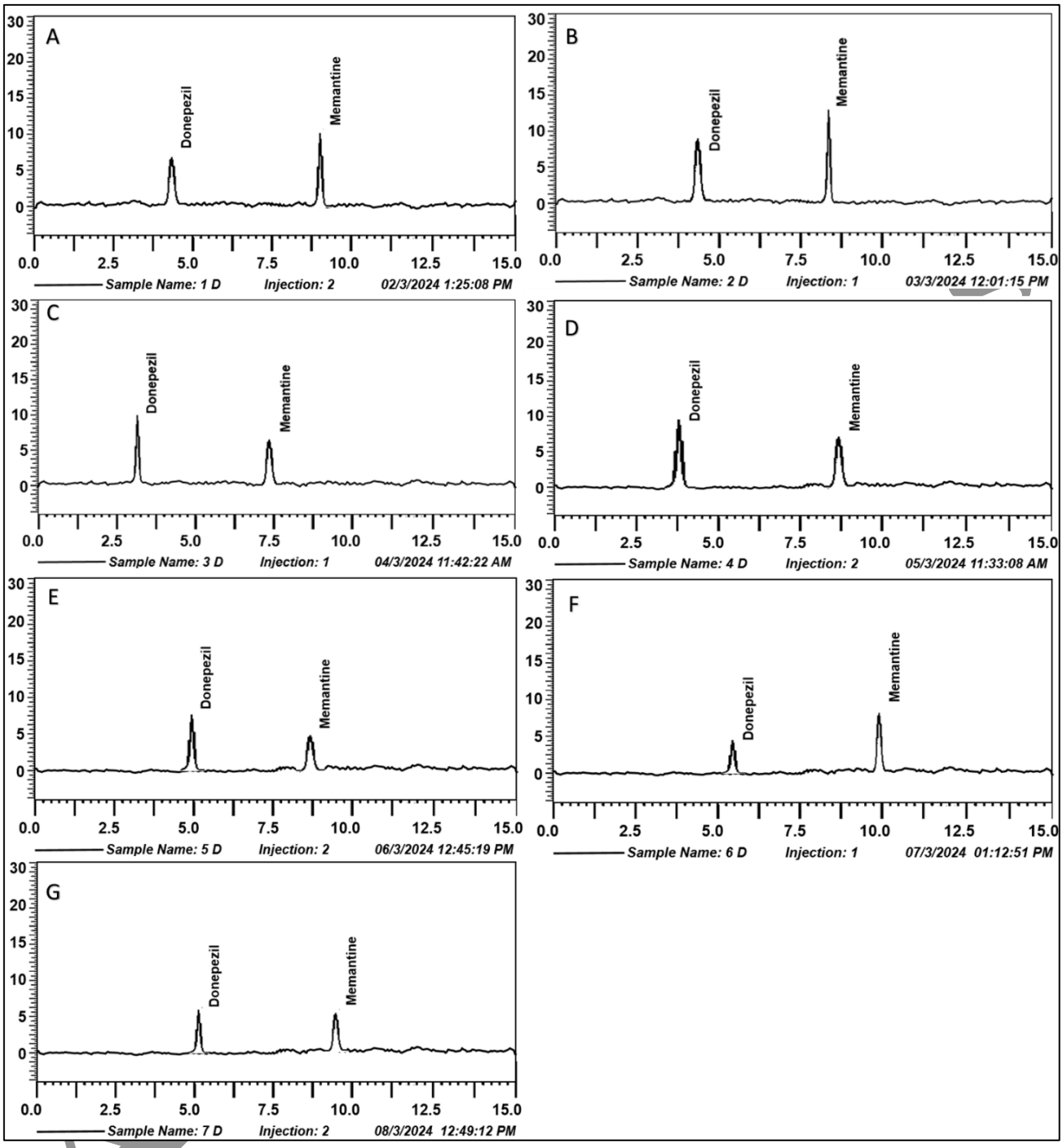


Fig. 9: The chromatogram of the plasma sample on (A) day 1; (B) day 2; (C) day 3; (D) day 4; (E) day 5; (F) day 6; (G) day 7 with TDP-11.

Non-nominal variations in weight, thickness, pH and drug content are observed to exhibit a strong and reproducible manufacturing process. Differences in the patterns of moisture behavior, flux and permeability are manifestations of the extent to which polymer ratios and plasticizer contents modulate matrix porosity and drug-diffusion properties. Among the high-flow formulations, especially TDP-11, the one with excellent mechanical properties, low moisture absorption and high permeation efficiency was selected as the best formulation.

The relatively poorer fit to first-order kinetics suggested that the release is not only diffusion-controlled by the concentration gradient within the matrix but is also highly influenced by the structural changes in the polymeric film (Venkatesh *et al.*, 2024). Strong linearity for both the Higuchi and Korsmeyer-Peppas models indicated the importance of diffusion through a swollen matrix and confirmed that water uptake and polymer relaxation are critical steps in regulating drug transport.

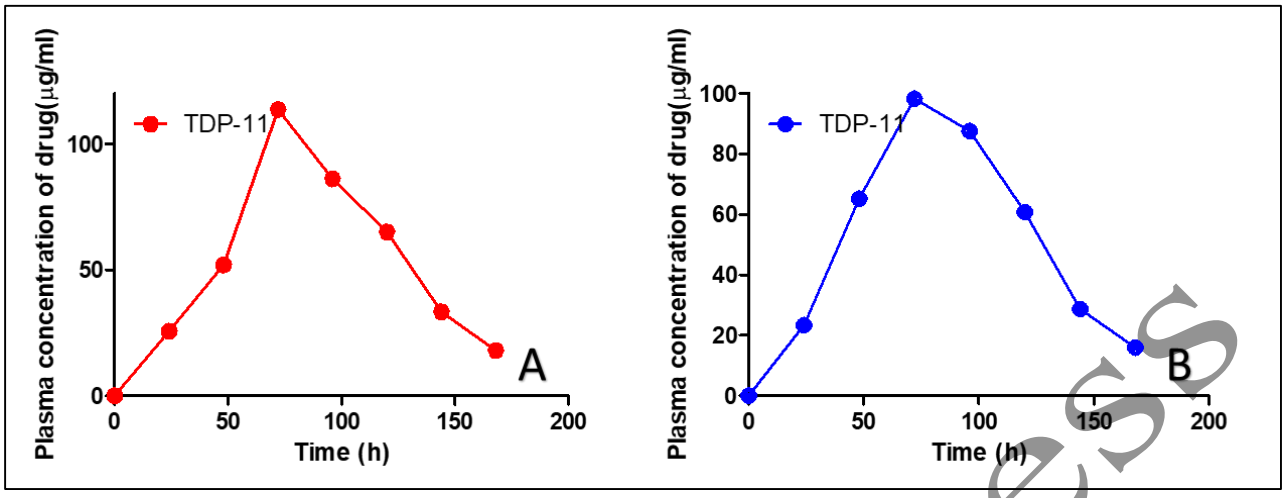


Fig. 10: *In-vivo* donepezil and memantine reachability from the transdermal patches in a rabbit model.

Parameter	Value	
	Donepezil	Memantine
AUC_{0-168} (µg·hr/L)	9235.44	8927.76
$AUMC_{0-168}$ (µg·hr²/L)	808352.64	766673.28
Cmax (µg/L)	113.64	98.27
Tmax (h)	72	72
Elimination rate constant (Kel) (h-1)	0.02238	0.02445
Half-life (t½) (h)	30.97	28.35
$AUC_{0-\infty}$ (µg·hr/L)	10038.87	9578.79
$AUMC_{0-\infty}$ (µg·hr²/L)	943329.54	876045.70
Mean residence time (MRT) (h)	93.97	91.46

Such control over the general rate by gradual erosion or dissolution of the matrix, coupled with a reduction in overall effective surface area, would characterize the Hixson-Crowell model as an ideal release mechanism (Kiran *et al.*, 2025). Typical of hydrophilic polymeric transdermal systems, this combined diffusion-erosion mechanism should provide evidence of the suitability of the optimized formulation for sustained drug delivery, nearly constant throughout the period for which it is intended to be used. This slightly lower fit to the Hixson-Crowell suggests that erosion or structural alteration of the matrix does occur during hydration, although this is not the factor that predominantly controls MMT release (Dinh *et al.*, 2022).

The Figures for erythema and edema are very low and declining, suggesting that the polymers, plasticizers and all other excipients chosen for the patch are dermatologically acceptable and do not compromise the integrity of the skin barrier with prolonged applications or contact. With chronic therapies, such as transdermal delivery of CNS drugs, especially when using patches for long durations, cumulative irritation can be a hindrance to patient adherence. These effects confirm that the optimized formulation can be applied to the skin for several hours without clinically relevant irritation or sensitization. Thus, skin tolerability data are sufficient to support further developmental studies and to justify proceeding to longer-term safety and efficacy evaluations in the appropriate animal model or clinical studies (Dighe *et al.*, 2023).

A smooth, defect-free matrix with controlled porosity would therefore be the best support for transdermal delivery systems, as it strikes a balance between mechanical strength and efficient permeation. Together with physicochemical and permeation data, the SEM results corroborate that TDP-11 has a well-optimized microstructure for sustained, controlled delivery of DPZ and MMN over a long period (Tuna *et al.*, 2025). Hence, the morphology observed substantiates the formulation as a good, reliable and effective platform for transdermal treatment and serves as a basis for further progression to *in-vivo* performance and stability evaluations.

Upon examination of stability, it was found that the polymer matrix and plasticizers protect the DPZ and MMN from heat degradation and humidity while maintaining integrity, the drug release profile and skin compatibility (Satheesh Kumar *et al.*, 2025). Under stressed conditions, mechanical properties, surface pH and drug content uniformity were found to be satisfactory, suggesting that the patches will be well-accepted in terms of shelf life for

Article in Press

extended transdermal therapy with controlled dosage, thereby improving patient adherence compared to oral administration (Ali *et al.*, 2024). The potential erosion of mechanical properties and individual surfaces' pH, which contribute to patient handling characteristics and dermal tolerability, will indeed continue to be good over a long period, hence greatly useful in chronic-use transdermal therapy.

The decrease in peak areas from day 5 to day 7 indicates reservoir depletion, demonstrating that the patch remains functional for 7 days from the time of application and confirming its once-weekly formulation. In addition, the retention times remain consistent and there are no hindering peaks, indicating selective retention and confirming the chemical stability of the parent drug during transdermal administration and systemic circulation (Abdul Ahad *et al.*, 2025). Taken together, these observations, both *in-vivo* and chromatographic, show that TDP-11 has the desired profile of a controlled-release transdermal system with prolonged, predictable exposure with a convenient weekly application (Khan *et al.*, 2025).

Upon substitution with TDP-11, plasma donepezil levels rose over time and reached a maximum around 72 h; thereafter, levels decreased gradually over the subsequent hours up to 168 h, indicating controlled and sustained release of the drug over time (Nikhil Kumar *et al.*, 2025). The values from the AUC_{0-168} and $AUMC_{0-168}$ suggest prolonged systemic exposure, an extended mean residence time and thus effective transdermal absorption for a period of seven days. Thus, the results indicate that TDP-11 could provide therapeutically effective plasma concentrations with once-weekly dosing, preventing peak-trough fluctuations and improving patient adherence compared with multiple daily oral administrations (Cunha *et al.*, 2021). Plasma levels-time data following transdermal administration provided the basis for conducting the pharmacokinetic study of the formulation tested. The non-compartmental methods and estimation (trapezoidal rule) were considered in calculating key parameters, which included AUC, AUMC, C_{max}, t_{max}, elimination rate constant (Kel), half-life ($t_{½}$), AUC at infinite dose ($AUC_{0-\alpha}$), AUMC at infinite dose ($AUMC_{0-\alpha}$) and the mean residence time (MRT). The drug exhibited a slow buildup of plasma concentration to the maximum concentration (t_{max}), followed by a steady decrease, which supported the use of the extended-release formulation (Mo *et al.*, 2022).

This means that the difference in drug absorption during the sampling period is negligible, at about 8.7%. This demonstrates the greatest drug absorption during the sampling period, thereby confirming the reliability of systemic exposure measurements. The AUMC of the first moment and an extrapolated area were 808352.64 and 943329.54 µg•hr^2/L, respectively (Witika *et al.*, 2022). Based on these values, the mean residence time (MRT) was 93.97 h, indicating that the drug will remain in the systemic circulation, which is beneficial for avoiding frequent dosing to achieve the therapeutically effective level (Mohan *et al.*, 2025).

CONCLUSION

The study concludes that first-pass metabolism, variable plasma drug levels, adverse effects related to doses and poor adherence limit conventional oral therapy for Alzheimer's disease, especially in Alzheimer's disease patients. In this study, a transdermal drug delivery system has been developed and *in-vivo* evaluated for Memantine (MMT) and Donepezil (DPZ)-loaded transdermal films, demonstrating it as a good alternative. Formulated with PVP K30, modified chitosan and HPMC K15, the optimized patch (TDP-11) was selected based on comprehensive *in-vitro* and *in-vivo* assessments. Pharmacokinetic evaluation in healthy rabbits confirmed prolonged drug release, enhanced bioavailability and sustained systemic exposure, with TDP-11 exhibiting favorable physicochemical properties, higher and more consistent C_{max} values and a prolonged t_{max} of 6 h, indicative of controlled and sustained drug delivery. The findings establish that the optimized transdermal films provide superior pharmacokinetic performance compared to conventional oral administration and represent a promising, patient-friendly therapeutic approach with the potential to improve adherence, reduce dosing frequency and enhance treatment efficacy in patients with Alzheimer's disease.

Acknowledgments
None.

Author's contributions
Bariki Rajasekhar conceived and designed the study, performed the experimental work, collected and analyzed the data and drafted the manuscript. Haranath Chinthaginjala contributed to the study design, supervised the research work, validated the results and critically reviewed and edited the manuscript. Both authors read and approved the final manuscript.

Funding
Self funding

Data availability statement
Data available upon request to the corresponding author.

Ethical approval
Institutional Animal Ethics Committee (RIPA/2020/COL-19R) approval was sought for experimentation. For conducting animal experiments, CPCSEA (No. 855/ac/05/CPCSEA/009/2021) has approved the

Article in Press

institution. This study was performed in adherence with the ARRIVE guidelines. See supplementary file for the ARRIVE checklist.

Conflict of interest

The authors declare that they have no known competing financial interests or personal relationships that could have appeared to influence the work reported in this paper.

REFERENCES

Abdul Ahad H, SP R, Sugali Banoth T and Ganugapenta NK (2025). Development and *in-vitro* characterization of a HPMC K4M and guar gum-based triple-layer matrix tablet system for chondroitin sulphate and diclofenac sodium. *Bull. Pharm. Sci. Assiut Univ.* **48** (2): P859-873.

Ahad HA, Dheeraj S and Chinthaginjala H (2023). Enhancing anti-allergic transdermal patches through box-behnken design approach with chlorpheniramine maleate. *Int. J. Life Sci. Pharma Res*, **13**(6): P366-377.

Akhlaq M, Arshad MS, Mudassir AM, Hussain A, Kucuk I, Haj-Ahmad R and Ahmad Z (2016). Formulation and evaluation of anti-rheumatic dexibuprofen transdermal patches: A quality-by-design approach. *J. Drug Target*, **24**(7): P603-612.

Ali MH, Alam O, Ali A, Ali MU, Parvez S, Aldosari E and Ali J (2024). Donepezil and embelin loaded nanostructured lipid carriers for direct brain delivery as an intervention for alzheimer's disease: Formulation design, optimization and evaluation. *J. Clust. Sci.* **35**(4): P1021-1044.

Altun E, Yuca E, Ekren N, Kalaskar DM, Ficai D, Dolete G and Gunduz O (2021). Kinetic release studies of antibiotic patches for local transdermal delivery. *Pharmaceutics*, **13**(5): P613.

Amena SN and Rizwan SH (2015). Stability-indicating analytical method development and validation of memantine and HCl and donepezil HCl using RP-HPLC. *Int J Pharm Pharm Sci*, **7**(11): P204-210.

Aminisaman J, Nazari J and Kavyannejad R (2025). Effects of co-administration of fentanyl and nitroglycerin on hemodynamic responses during intubation and extubation: A randomized clinical trial. *J. Perianesth. Nurs.* **40**(3): P579-585.

Angelopoulou E, Paudel YN, Papageorgiou SG and Piperi C (2021). APOE genotype and Alzheimer's disease: The influence of lifestyle and environmental factors. *ACS Chem. Neurosci.*, **12**(15): P2749-2764.

Arora P and Mukherjee B (2002). Design, development, physicochemical and *in-vitro* and *in-vivo* evaluation of transdermal patches containing diclofenac diethylammonium salt. *J. Pharm. Sci.* **91**(9): P2076-2089.

Bácskay I, Hosszu Z, Budai I, Ujhelyi Z, Feher P, Kosa D and Peto A (2023). Formulation and evaluation of transdermal patches containing BGP-15. *Pharmaceutics*, **16**(1): P1-36.

Bai J, Lu Y, Li PY, Liu CM, Wu HC, Wen R and Du SY (2014). Development and *In-vitro* evaluation of a transdermal hydrogel patch for ferulic acid. *Pak. J Pharm. Sci*, **27**(2): P369-375.

Bhushan I, Kour M, Kour G, Gupta S, Sharma S and Yadav A (2018). Alzheimer's disease: Causes and treatment–A review. *Ann Biotechnol*, **1**(1): P1-8.

Buck A, Rezaei K, Quazi A, Goldmeier G, Silverglate B and Grossberg GT (2024). The donepezil transdermal system for the treatment of patients with mild, moderate, or severe Alzheimer's disease: A critical review. *Expert Rev. Neurother.***24**(6): P607-614.

Cunha S, Forbes B, Sousa Lobo JM and Silva AC (2021). Improving drug delivery for Alzheimer's disease through nose-to-brain delivery using nanoemulsions, nanostructured lipid carriers (NLC) and *in situ* hydrogels. *Int. J Nanomed*, **29** (16): P4373-4390.

Davanco MG, Fortuny M, Scasso A, Meulman J, Costa F, da Silva TM and Sampaio ACC (2024). Buprenorphine transdermal delivery system: Bioequivalence assessment and adhesion performance of two patch formulations. *Pharmaceutics*, **16**(10): P1249.

Dighe S, Jog S, Momin M, Sawarkar S and Omri A (2023). Intranasal drug delivery by nanotechnology: Advances in and challenges for Alzheimer's disease management. *Pharmaceutics*, **16**(1): P16-58.

Dinh L, Lee S, Abuzar SM, Park H and Hwang SJ (2022). Formulation, preparation, characterization and evaluation of dicarboxylic ionic liquid donepezil transdermal patches. *Pharmaceutics*, **14**(1): P205-225.

Egunlusi AO and Joubert J (2024). NMDA receptor antagonists: Emerging insights into molecular mechanisms and clinical applications in neurological disorders. *pharmaceuticals*, **17**(5): P639.

Ertas B, Onay IN, Yilmaz-Goler AM, Karademir-Yilmaz B, Aslan I and Cam ME (2023). A novel high-efficiency transdermal patch for combinational therapy of Alzheimer's disease: Donepezil/vitamin B12-loaded nanofibers. *J. Drug Del. Sci. Tech*, **89**: P104963.

Falcone D, Spee P, Salk K, Peppelman M, Van De Kerkhof P and Van Erp P (2017). Measurement of skin surface biomarkers by transdermal analysis patch following different *in-vivo* models of irritation: A pilot study. *Skin Res. Tech*, **23**(3): P336-345.

Ghosh M and Banga AK (2025). Formulation and evaluation of a transdermal drug-in-adhesive patch for lamotrigine delivery in potential epilepsy treatment. *J. Drug Del. Sci. Tech.*, P107067.

Javed S, Mangla B, Almoshari Y, Sultan MH and Ahsan W (2022). Nanostructured lipid carrier system: A compendium of their formulation development approaches, optimization strategies by quality by design and recent applications in drug delivery. *Nanotechnol. Rev*, **11**(1): P1744-1777.

Article in Press

Jiang Y, Murnane KS, Bhattacharjee SA, Blough BE and Banga AK (2019). Skin delivery and irritation potential of phenmetrazine as a candidate transdermal formulation for repurposed indications. *AAPS J.* **21**(4): P70.

Kajal Sharma DR, Pandit V and Ashawat M (2024). Formulation and evaluation of niosomal loaded transdermal patches for the treatment of osteoarthritis. *Drug Del. Lett,* **14**(4): P290-307.

Khan SA, Qamar Z, Rohilla A, Singh PP, Parvez S, Baboota S and Ali J (2025). Prospective utilization of nanocarriers loaded with drug combination for treating Alzheimer's disease. *Cur. Pharm. Des*. **31**(18):P1444-1460.

Kharia A, Singhai A and Gilhotra R (2020). Formulation and evaluation of transdermal patch for the treatment of inflammation. *J. Pharm. Sci. Res.*, **12**(6): P780-788.

Khire A and Vavia P (2014). Bioavailability, bioequivalence and *in-vitro–in-vivo* correlation of oxybutynin transdermal patch in rabbits. *Drug Del. Transl. Res.,* **4**(2): P105-115.

Kim EJ and Choi DH (2021). Quality by design approach to the development of transdermal patch systems and regulatory perspective. *J. Pharm. Inv,* **51**(6): P669-690.

Kim S, Youssef SH, Lee KMK, Song Y, Vaidya S and Garg S (2024). Enhanced skin permeation of 5-fluorouracil through drug-in-adhesive topical patches. *Pharmaceutics,* **16**(3): P379.

Kiran NS, Vaishnavi G, Singh S, Yashaswini C, Parihar A, Pal S and Puri A (2025). Biomaterials comprising implantable and dermal drug delivery targeting the brain in management of Alzheimer's disease: A review. *Regener. Eng. Transl. Med.* **11**(1): P15-38.

Koppa Raghu P, Bansal KK, Thakor P, Bhavana V, Madan J, Rosenholm JM and Mehra NK (2020). Evolution of nanotechnology in delivering drugs to eyes, skin and wounds via topical route. *Pharmaceuticals,* **13**(8): P167.

Kumar LS and Ahad HA (2023). Quality by design based quercetin hydrate nanoemulsions for enhanced solubility by reducing particle size. *Indian J. Pharm. Educ. Res.* **57**(4): P965-970.

Lei Y, Yang G, Du F, Yi J, Quan L, Liu H and Wang Y (2022). Formulation and evaluation of a drug-in-adhesive patch for transdermal delivery of colchicine. *Pharmaceutics,* **14**(10): P2245.

Matsunaga S, Kishi T, Nomura I, Sakuma K, Okuya M, Ikuta T and Iwata N (2018). The efficacy and safety of memantine for the treatment of Alzheimer's disease. *Expert Opin. Drug Saf.* **17**(10): P1053-1061.

Milanifard M and Ramezani M (2025). Clinical and neurological problems and clinical tests in Alzheimer's patients specializing in Alzheimer's disease. *Eur. J. Chem. Med. Pet. Res.* **4**(2): P152-163.

Mo L, Lu G, Ou X and Ouyang D (2022). Formulation and development of novel controlled-release transdermal patches of carvedilol to improve bioavailability for the treatment of heart failure. *Saudi J. Biol. Sc*, **29**(1): 266-272.

Mohan N, Nair RPAN and Narayanasamy D (2025). Nanoparticle- integrated transdermal patches: A platform for next- generation drug delivery. *Drug Dev. Res*, **86**(7): e70164.

Momin Z, BPK, KVB and Kumar L (2025). Formulation, characterization and evaluation of transdermal patches of ranolazine for chronic angina pectoris. *Naunyn-Schmiedebergs Arc. Pharmacol*, **399**(2): P2227-2242.

Nikhil Kumar G, Satheesh Kumar E, Banoth TNS, Sugunarajan Latha A, Melehalli Shivaraju B and Abdul Ahad H (2025). Harnessing liposome technology for precision medicine: Design, delivery and clinical impact. *Nanomed. J.* **13**(2): P283-295,

Nunes D, Tavares TG, Malcata FX, Loureiro JA and Pereira MC (2024). Development and validation of a simple UV–HPLC method to quantify the memantine drug used in Alzheimer's treatment. *pharmaceuticals,* **17**(9): P1162.

Otterbach A and Lamprecht A (2021). Enhanced skin permeation of estradiol by dimethyl sulfoxide containing transdermal patches. *Pharmaceutics,* **13**(3): P320.

Parhi, R and Padilam, S. (2018). *In-vitro* permeation and stability studies on developed drug-in-adhesive transdermal patch of simvastatin. *Bull. Fac. Pharm. Cairo Univ.*, **56**(1): P26-33.

Qadir A, Jan SU, Shoaib MH, Sikandar M, Yousuf RI, Ali FR and Saleem MT (2025). Formulation development and evaluation, *in silico* PBPK modeling and *in-vivo* pharmacodynamic studies of clozapine matrix type transdermal patches. *Sci.Rep,* **15**(1): P1204.

Sabareesh M, Rajangam J, Prakash Raj K and P Yanadaiah J (2024). Formulation and evaluation of novel vesicular nanoethosomal patches for transdermal delivery of zidovudine: *In-vitro*, *ex-vivo* and *in-vivo* pharmacokinetic investigations. *J. Disp. Sci. Tech*, P1-14.

Safiri S, Ghaffari Jolfayi A, Fazlollahi A, Morsali S, Sarkesh A, Daei Sorkhabi A and Hamidi S (2024). Alzheimer's disease: A comprehensive review of epidemiology, risk factors, symptoms, diagnosis, management, caregiving, advanced treatments and associated challenges. *Front. Med*, **11**: 1474043.

Sailaja C and Bhupalam PK (2025). Optimizing loratadine delivery: Development of niosomal transdermal patches. *Indian J.Pharm. Edu. Res.*, **59**(2s): Ps443-s453.

Satheesh Kumar E and Ahad HA (2025). *In-vivo* pharmacokinetic evaluation of a gastro-retentive triple drug delivery system utilizing natural polymers for enhanced *Helicobacter pylori* eradication. *Bull. Fac. Pharm. Cairo Univ*, **63**(2): P49-57.

Scheltens P, De Strooper B, Kivipelto M, Holstege H, Chetelat G, Teunissen CE and van der Flier WM (2021). Alzheimer's disease. *The Lancet*, **397**(10284): P1577-1590.

Article in Press

Sharma PK, Panda A, Pradhan A, Zhang J, Thakkar R, Whang CH and Murthy SN (2018). Solid-state stability issues of drugs in transdermal patch formulations. *AAPS PharmSciTech*, **19**(1): P27-35.

Shivalingam M, Balasubramanian A and Ramalingam K (2021). Formulation and evaluation of transdermal patches of pantoprazole sodium. *Int J App Pharm*, **13**(5): P287-291.

Singh A and Bali A (2016). Formulation and characterization of transdermal patches for controlled delivery of duloxetine hydrochloride. *J. Anal. Sci. Tech.*, **7**(1): P7-25.

Tuna RW, Achmad NA, Kurniawan I, Khairiyah Asaf MB, Sapiun Z and Permana AD (2025). Development of thermosensitive mucoadhesive gel-incorporated lipid microspheres of donepezil for enhanced nose-to-brain delivery. *J.Biomat. Sci., Poly. Edi*, **36** (15): P2159-2186.

Venkatesh R, Ahad HA and Kumar ES (2024). Optimization of vildagliptin delivery: Formulation and evaluation using box-behnken design. *Res. J. Pharm. Tech*, **17**(12): P5923-5930.

Winblad B, Kilander L, Eriksson S, Minthon L, Batsman S, Wetterholm AL and Haglund A (2006). Donepezil in patients with severe Alzheimer's disease: Double-blind, parallel-group, placebo-controlled study. *The Lancet*, **367**(9516): P1057-1065.

Witika BA, Poka MS, Demana PH, Matafwali SK, Melamane S, Malungelo Khamanga SM and Makoni PA (2022). Lipid-based nanocarriers for neurological disorders: A review of the state-of-the-art and therapeutic success to date. *Pharmaceutics*, **14**(4): P836.

Wong WF, Ang KP, Sethi G and Looi CY (2023). Recent advancement of medical patch for transdermal drug delivery. *Medicina*, **59**(4): P778.

Yadav PK and Mishra S (2017). Transdermal patch of an antihypertensive drug: Its development and evaluation. *World J. Pharm. Res*, **6**(4): P1355-1374.

Zhang T, Liu C, Zhong N, Wang Y, Huang Y and Zhang X (2024). Advances in the treatment of cognitive impairment in schizophrenia: Targeting NMDA receptor pathways. *Int. J. Mol. Sci*, **25**(19): P10668.

Article in Press